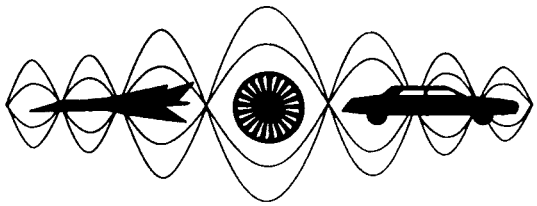

FIFTH INTERNATIONAL CONGRESS ON SOUND AND VIBRATION
DECEMBER 15-18, 1997
ADELAIDE, SOUTH AUSTRALIA

CHARACTERISTICS OF CHIRAL SLAB IN THE APPLICATIONS OF WAVE ABSORPTION

Sung Chia-Chi* Ro Ruyen** Yuh-Ming Chang*

* Department of Naval Architecture and Ocean Engineering National Taiwan University
**Department of Electrical Engineering I-Shou University

ABSTRACT

Acoustically active materials (chiral materials) that lack centrosymmetry due to chirality in their microstructures can be characterized by the constitutive relations $\sigma_{ji} = \mu\gamma_{ji} + \mu\gamma_{ij} + \lambda\gamma_{kk}\delta_{ij} + c\kappa_{ji}$ and $\chi_{ji} = (\xi + \varepsilon)\kappa_{ji} + (\xi - \varepsilon)\kappa_{ij} + \eta\kappa_{kk}\delta_{ij} + c\gamma_{ji}$. Accordingly, two longitudinally, two right circularly and two left circularly polarized elastic waves can propagate in chiral medium. Using appropriate field representations along with prescribed boundary conditions, scattering characteristics at chiral interfaces can be realized. In this paper, reflection and transmission characteristics of chiral slabs bounded by achiral media for longitudinally elastic waves with normal incident are thoroughly discussed. Results obtained can be applied for the design of broadband acoustic impedance transformer and acoustic absorbers which will be reported in the near future.

1. INTRODUCTION

Chiral materials, which lack inversion symmetry due to handedness in their microstructure, have been known and called optically active materials in theoptical spectrum since the beginning of last century.[2, 4] Circularly polarized waves are eigenstates in chiral media.[12] Because of different in chiral media[12]. Because of different propagation characteristics of left circularly polarized (LCP) and right circularly polarized (RCP) waves in chiral materials, circular dichroism (CD)[14] and optical rotatory dispersion (RD)[6] may be measured and adopted to characterize chiral materials. Although chirality is chiefly known at optical frequencies, electromagnetic activities can bemeasured from artificial chiral composites at microwave frequencies.[8, 13] The handedness of objects detected in the optical and electromagnetic spectra results from the transverse nature of optical and electromagnetic waves.[1] It follows that elastic waves, which consist of longitudinal and transverse components, may be capable of sensing the handedness of objects at acoustic frequencies. Dispersion equations and field equations for elastic waves propagating in chiral materials can be obtained by using constitutive relations[3, 11] and governing equations[7] for noncentrosymmetric,

isotropic micropolar materials.[5, 9] Accordingly, two longitudinally, two right circularly and two left circularly polarized elastic waves can propagate in chiral medium.

In order to solve elastic wave problems involving contiguous regions of different constitutive parameters, it is necessary to know the boundary conditions that vector and stress fields must satisfy at the interfaces. It can be shown that boundary conditions at chiral-chiral interfaces are uniquely defined by applying principles of conservation of forces and momenta.[5] Consequently, scattering characteristics at chiral-chiral interfaces are uniquely obtained. The effects of the constitutive parameters of chiral materials on reflection characteristics for elastic waves normally impinging upon achiral-chiral interfaces are elucidated by appropriate boundary conditions.[10] It is illustrated that reflection coefficients may vanish by properly tailoring constitutive parameters of chiral materials. In addition, the methods for determining constitutive parameters of chiral materials for zero reflection at achiral-chiral interfaces are established. Continuing with previous studies, reflection and transmission characteristics of chiral slabs bounded by achiral media for longitudinally elastic waves with normal incidence are investigated in this paper. Results obtained can be used to analyze multiple chiral layers' problems as well as further to tailor acoustic materials using chiral composites.

2. THEORY

For normally incident longitudinal elastic waves, field representations for the planar chiral slab bounded by achiral media can be illustrated by Fig. 1. There are three regions in Fig. 1. Two of them, region 1 ($z \leq 0$) and region 3 ($z \geq d$), are achiral media, which can be characterized by Lamé constants λ and μ. In addition to Lamé constants, micropolar elastic constants ξ and η, and the constant c associated with noncentrosymmetry are constitutive parameters for chiral medium, region 2 ($0 \leq z \leq d$).[9, 10]

In region 1, elastic fields which consist of incident and reflected fields can be represented as

$$\mathbf{u}^1 = \mathbf{u}^{inc} + \mathbf{u}^{ref} = \mathbf{a}_z\left(A^t e^{ik_1 z} + A^r e^{-ik_1 z}\right) \tag{1}$$

where k_1 is the longitudinal wavenumber in region 1. The transmitted fields in region 3 take the form

$$\mathbf{u}^3 = \mathbf{u}^{tra} = \mathbf{a}_z\left(A^t e^{ik_3 z}\right) \tag{2}$$

where k_3 is the longitudinal wave number in region 3. In the chiral medium, region 2, elastic fields, which consist of displacement and rotation fields, propagating in both the positive and negative z-directions can be represented as

$$\begin{aligned}\mathbf{u}^2 &= \mathbf{u}^{2+} + \mathbf{u}^{2-} \\ &= \mathbf{a}_z\left(B_1 e^{ik_{L1} z} + B_2 e^{ik_{L2} z} + B_3 e^{-ik_{L1} z} + B_4 e^{-ik_{L2} z}\right)\end{aligned} \tag{3}$$

$$\begin{aligned}\varphi^2 &= \varphi^{2+} + \varphi^{2-} \\ &= \mathbf{a}_z\left(R_{L1} B_1 e^{ik_{L1} z} + R_{L2} B_2 e^{ik_{L2} z} + R_{L1} B_3 e^{-ik_{L1} z} + R_{L2} B_4 e^{-ik_{L2} z}\right)\end{aligned} \tag{4}$$

where u is the displacement vector and φ is the rotation vector. The wavenumbers k_{L1} and k_{L2} which represent longitudinal waves in chiral media can be numerically solved from the following equation[9)]

$$k^4\left(1-J\beta^2 k_L{}^2 k_{RL}{}^2\right)-k^2\left(k_L{}^2+k_{RL}{}^2\right)+k_L{}^2 k_{RL}{}^2=0 \tag{5}$$

where J is the angular momentum, $k_L = \omega/[(\lambda_2 + 2\mu_2)/\rho_2]^{1/2}$, $k_{RL} = \omega/[(\eta_2 + 2\xi_2)/J\rho_2]^{1/2}$, and $\beta = c/J\rho_2\omega^2$ are shorthand notations. The ratios of the rotation vector to the displacement vector, R_{L1} and R_{L2}, can be determined by substituting $k_{L1} = k$ and $k_{L2} = k$ into the following eqation[9)]

$$R_L=\left(1-k^2/k_L{}^2\right)/J\beta k^2=\beta k^2/\left(1-k^2/k_{RL}{}^2\right) \tag{6}$$

By applying principles of conservation of forces and momenta, boundary conditions for normally incident longitudinal waves at achiral-chiral interfaces can be uniquely determined as given by[12, 14)]

$$\mathbf{a}_z\bullet\left(\mathbf{u}^1-\mathbf{u}^2\right)\Big|_{z=0}=0,\ \mathbf{a}_z\bullet\left(\mathbf{u}^2-\mathbf{u}^3\right)\Big|_{z=d}=0 \tag{7}$$

$$\left(\sigma_{zz}^1-\sigma_{zz}^2\right)\Big|_{z=0}=0,\ \left(\sigma_{zz}^2-\sigma_{zz}^3\right)\Big|_{z=d}=0 \tag{8}$$

$$\left(\chi_{zz}^2\right)\Big|_{z=0,d}=0 \tag{9}$$

Equations (7) and (8) indicate continuities of normal components of displacement fields and force stresses, respectively. The third boundary condition, Eq. (9), illustrates that the normal component of the couple stress must vanish at achiral-chiral interfaces. The force stress σ_{zz} in Eq. (8) and the couple stress χ_{zz} in Eq. (9) can be determined from the constitutive relations as given by

$$\sigma_{zz}^1=\left(2\mu_1+\lambda_1\right)u_{z,z}^1 \tag{10}$$

$$\sigma_{zz}^2=\left(2\mu_2+\lambda_2\right)u_{z,z}^2+c\varphi_{z,z}^2 \tag{11}$$

$$\sigma_{zz}^3=\left(2\mu_3+\lambda_3\right)u_{z,z}^3 \tag{12}$$

$$\chi_{zz}^2=\left(2\xi+\eta\right)\varphi_{z,z}^2+cu_{z,z}^2 \tag{13}$$

The unknown constants, A^r, A^t, B_1, B_2, B_3, and B_4 can be determined in terms of A^i by enforcing boundary conditions at achiral-chiral interfaces. Substituting field representations, Eqs. (1)-(4), and constitutive relations, Eqs. (10)-(13), into boundary conditions, Eqs. (7)-(9) yields the following equation

$$\begin{bmatrix} -1 & 1 & 1 & 1 & 1 & 0 \\ 0 & e^{ik_{L1}d} & e^{-ik_{L1}d} & e^{ik_{L2}d} & e^{-ik_{L2}d} & -1 \\ Z_1 & M(3,2) & -M(3,2) & M(3,4) & -M(3,4) & 0 \\ 0 & e^{ik_{L1}d}M(3,2) & -e^{-ik_{L1}d}M(3,2) & e^{ik_{L2}d}M(3,4) & -e^{-ik_{L2}d}M(3,4) & -Z_3 \\ 0 & M(5,2) & -M(5,2) & M(5,4) & -M(5,4) & 0 \\ 0 & e^{ik_{L1}d}M(5,2) & -e^{-ik_{L1}d}M(5,2) & e^{ik_{L2}d}M(5,4) & -e^{-ik_{L2}d}M(5,4) & 0 \end{bmatrix} \begin{bmatrix} A^r \\ B_1 \\ B_3 \\ B_2 \\ B_4 \\ A^t \end{bmatrix} = \begin{bmatrix} 1 \\ 0 \\ Z_1 \\ 0 \\ 0 \\ 0 \end{bmatrix} A^i \qquad (14)$$

where $Z_1 = [\rho_1(\lambda_1 + 2\mu_1)]^{1/2}$ is the longitudinal wave impedance for media 1, $Z_3 = [\rho_3(\lambda_3 + 2\mu_3)]^{1/2}$ is the longitudinal wave impedance for media 3, $M(3, 2) = (Z_L/k_L + \beta Z_{RL}k_{RL}R_{L1})k_{L1}$, $M(3, 4) = (Z_L/k_L + \beta Z_{RL}k_{RL}R_{L2})k_{L2}$, $M(5, 2) = (R_{L1}Z_{RL}/k_{RL} + \beta Z_{RL}k_{RL})k_{L1}$, $M(5, 4) = (R_{L2}Z_{RL}/k_{RL} + \beta Z_{RL}k_{RL})k_{L2}$, $Z_L = [\rho_2(\lambda_2 + 2\mu_2)]^{1/2}$, and $Z_{RL} = [\rho_2 J(\eta + 2\xi)]^{1/2}$ are shorthand notations.

3. NUMERICAL RESULTS AND DISCUSSIONS

The parameters adopted in this paper for calculating scattering characteristics of the chiral slab bounded by achiral media are J, k_{RL}/k_L, $J\beta^2k_L^2k_{RL}^2$, Z_L, k_Ld and Z_3/Z_1. The value of Z_3/Z_1 is arbitrary chosen to be 3. The value of Z_L used for simulation in Figs. 2 – 8 is chosen to be $\sqrt{3}$. The simulation results presented in this paper are all plotted versus the nondimensional parameter k_Ld. The effects of the angular momentum J on the scattering characteristics are shown in Figs. 2 (a) and 2 (b). It can be seen clearly in these two figures that the reflection and transmission coefficients do not vary significantly with J in the k_Ld range of 1 to 360 (degree) while the rest parameters remain constant. Consequently, the value of J used in this paper is chosen, without loss of generality, to be 10. Reflection and transmission coefficients for the chiral slab with various values of $J\beta^2k_L^2k_{RL}^2$ and k_{RL}/k_L are plotted in Figs. 3-7. In these figures, curve 1, shown for comparison, represents either reflection or transmission coefficients of the quarter wavelength impedance transformer. This is achieved by letting region 2 be achiral medium with impedance $Z_2 = \sqrt{Z_1Z_3}$. For small values of $J\beta^2k_L^2k_{RL}^2$, e.g. 0.1, the chiral medium behaves almost like an achiral medium, which implies that displacement fields play major roles in the chiral medium. This is illustrated in Fig. 3 that curves 2, 3, and 4 resemble curve 1 excluding some special points. It is observed that reflection coefficient curves have a significant jump while transmission coefficients curves exhibit a corresponding drop at these special points. Further examination reveals that these phenomena occur when k_Ld approaches approximately multiples of $180°/(k_{RL}/k_L)$. At these points, the thickness of the chiral slab equals multiples of half wavelength for rotation fields and, hence, total reflection of rotation fields occurs. This contributes jumps and drops of reflection and transmission coefficient curves, respectively. As $J\beta^2k_L^2k_{RL}^2$ increases, rotation fields play somewhat more important roles and hence wave parameters of the chiral slab significantly change. This causes variations of magnitudes and locations of zero reflection and so does jumps and drops of reflection and transmission coefficients as shown in Figs. 4 and 5. As k_{RL}/k_L increases, wave parameters for the chiral slab vary significantly and, hence, reflection and transmission coefficient curves become more complex as can be seen in Figs. 6 and 7.

The normalized reflected, transmitted, and total powers with respect to the incident power are also computed for verification. Fig. 8 plots normalized powers for the chiral slab with

various values of $J\beta^2 k_L^2 k_{RL}^2$ and k_{RL}/k_L. Curves 1, 2, and 3 in this figure represent normalized reflected, transmitted and total powers, respectively. It is evident that conservation of energy is applied.

4. CONCLUSION

Using appropriate field representations along with prescribed boundary conditions, scattering characteristics of the chiral slab bounded by achiral media with the material parameters, Z_3/Z_1, J, k_L, k_{RL}/k_L, Z_L and $J\beta^2 k_L^2 k_{RL}^2$ can be realized. The reflection and transmission coefficients do not vary significantly with J in the $k_L d$ range of 1 to 360 (degree) while the rest parameters remain constant. With increasing either $J\beta^2 k_L^2 k_{RL}^2$ or k_{RL}/k_L the rotation fields play more important role and the wave parameters of the chiral slab vary significantly which cause the reflection and transmission phenomena much more complex. These results can be used for the design of broadband acoustic impedance transformers and acoustic absorbers which will be reported in the near future.

ACKNOWLEDGMENTS

The author would like to thank the National Science Council of the R.O.C. for financially supporting the research under the Contract No. NSC-85-2611-E-002-010.

REFERENCES

1. Bohren, C.F., (1974) *Chem. Phys.* Lett. 29 458.
2. J. Applequist: Am. Sci. 75 (1987) 59.
3. Lakes, R. S., and R. L. Benedict (1982) "Noncentrosymmetry in micropolar elasticity" *Int. J. Eng. Sci.* Vol. 20, pp. 1161-1167.
4. Lakhtakia, A., V.K. Varadan and V.V. Varadan (1989) "Time-Harmonic Electromagnetic Fields in Chiral Media" *Spring-Verlag*
5. Lakhtakia, A., V.K. Varadan and V.V. Varadan (1990) "Reflection of elastic plane wave at a planar achiral-chiral interface" *J. Acoust. Soc. Am.*, Vol. 87, pp. 2314-2318.
6. Lowry, T.M., 1935, *Optical Rotatory Power,* Logamans, Green and Co., New York
7. Nowacki, 1986, *Theory of Asymmetric Elasticity,* Pergamon Press, New York.
8. Ro, R., V.V. Varadan and V.K. Varadan (1992) "Electromagnetic activity and absorption in microwave chiral composites" *IEE Proc. H* Vol. 139, No. 5, pp. 441-448.
9. Ro, R. (1997) "Elastic wave propagation characteristics at chiral interface" *Jpn. J. Appl. Phys.*, Vol. 36 pp. 2253-2258.
10. Ro, R., and C. C. Sung (1997) "Parametric study of reflection characteristics at achiral-chiral interfaces" *Jpn. J. Appl. Phys.* 36.
11. Smith, A.C., (1967) "Waves in micropolar elastis solids" *Int. J. Eng. Sci.* Vol. 5, pp. 741-746.
12. Varadan, V.V., Varadan, A. Lakhtakia and V.V. Varadan (1988) "Equivalent dipole moments of helical arrangements of small, isotropic, point-polarizable scatters: Application to chiral polymer design" *J. Appl. Phys.* Vol. 63, pp. 280-284.
13. Varadan,V.V., R. Ro and V.K. Varadan (1994) "Measurement of the electromagnetic properties of chiral composite materials in the 8-40 GHz range" *Radio Sci.* Vol. 29, No. 1, pp. 9-22.
14. Velluz, L., 1965, *Optical Circular Dichroism*, Academic Press, New York

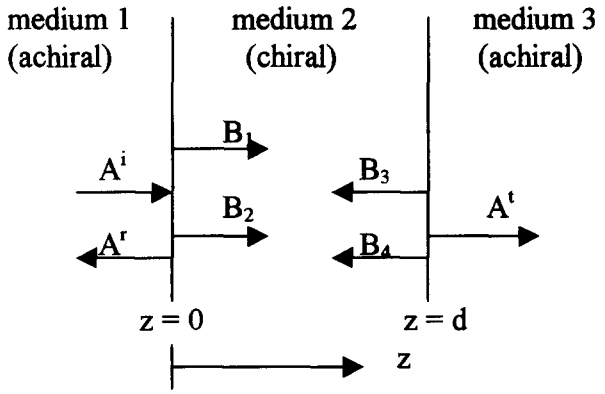

Fig.1 reflection and transmission of longitudinal waves normally incident on a planar chiral slab bounded by achiral media

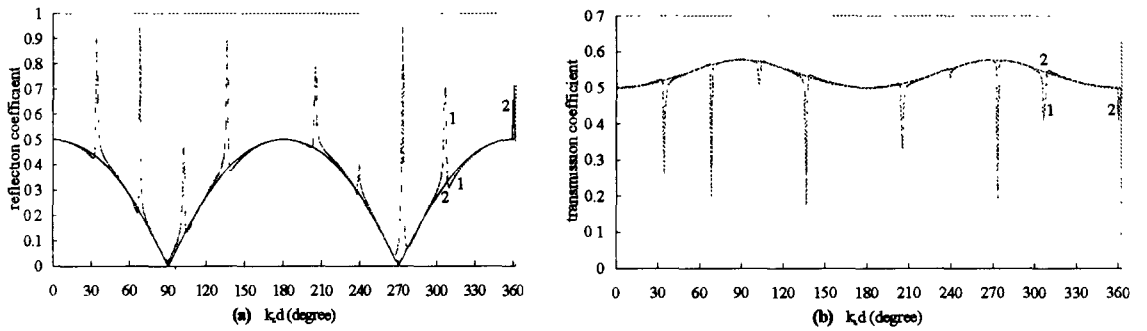

Fig.2 (a) reflection coefficient and (b) transmission coefficient for longitudinal waves normally incident on chiral medium with material constants: curve 1: $k_{RL}/k_L = 5$, $J\beta^2 k_L^2 k_{RL}^2 = 10^{-1}$, J = 1, 5 and 10 m^2, curve 2: $k_{RL}/k_L = 0.5$, $J\beta^2 k_L^2 k_{RL}^2 = 10^{-3}$, J = 1, 5 and 10 m^2

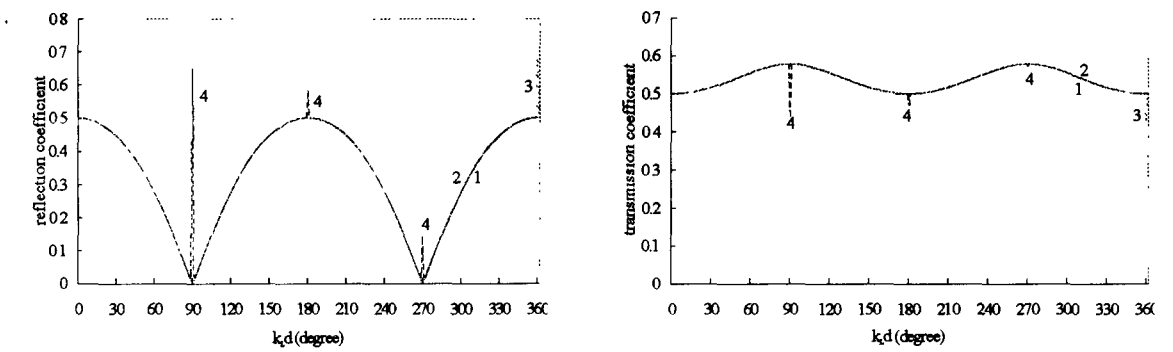

Fig.3 (a) reflection coefficient and (b) transmission coefficient for normally incident longitudinal waves versus $k_L d$, curve 1: region 2 being achiral medium with $Z_2 = \sqrt{Z_1 Z_3}$, curve 2: $J\beta^2 k_L^2 k_{RL}^2 = 10^{-3}$, $k_{RL}/k_L = 0.2$, curve 3: $J\beta^2 k_L^2 k_{RL}^2 = 10^{-3}$, $k_{RL}/k_L = 0.5$, curve 4: $J\beta^2 k_L^2 k_{RL}^2 = 10^{-3}$, $k_{RL}/k_L = 2$

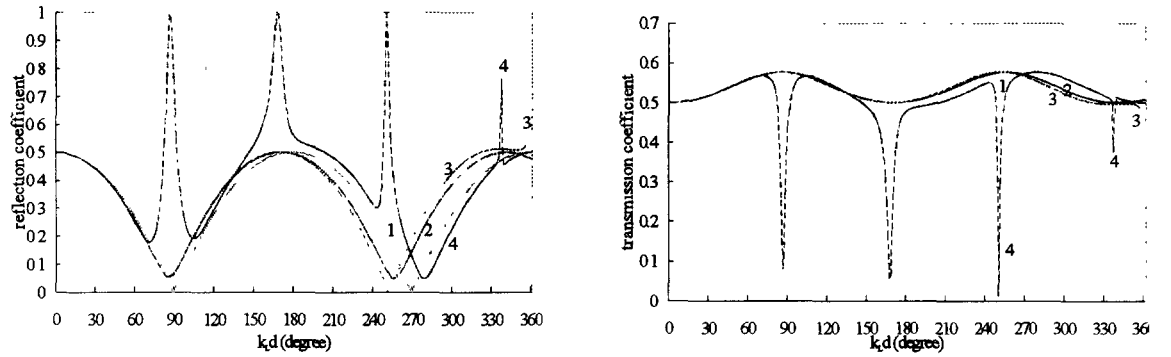

Fig.4 (a) reflection coefficient and (b) transmission coefficient for normally incident longitudinal waves versus k_Ld, curve 1: region 2 being achiral medium with $Z_2 = \sqrt{Z_1 Z_3}$, curve 2: $J\beta^2 k_L^2 k_{RL}^2 = 10^{-1}$, $k_{RL}/k_L = 0.2$, curve 3: $J\beta^2 k_L^2 k_{RL}^2 = 10^{-1}$, $k_{RL}/k_L = 0.5$, curve 4: $J\beta^2 k_L^2 k_{RL}^2 = 10^{-1}$, $k_{RL}/k_L = 2$

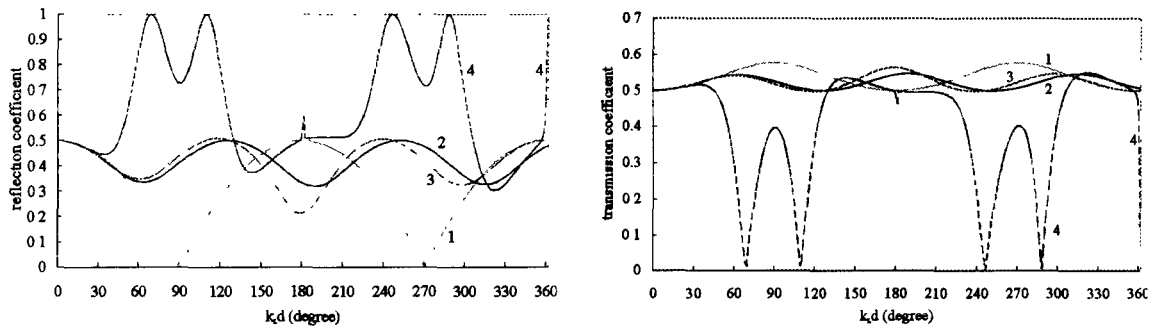

Fig.5 (a) reflection coefficient and (b) transmission coefficient for normally incident longitudinal waves versus k_Ld, curve 1: region 2 being achiral medium with $Z_2 = \sqrt{Z_1 Z_3}$, curve 2: $J\beta^2 k_L^2 k_{RL}^2 = 0.5$, $k_{RL}/k_L = 0.2$, curve 3: $J\beta^2 k_L^2 k_{RL}^2 = 0.5$, $k_{RL}/k_L = 0.5$, curve 4: $J\beta^2 k_L^2 k_{RL}^2 = 0.5$, $k_{RL}/k_L = 2$

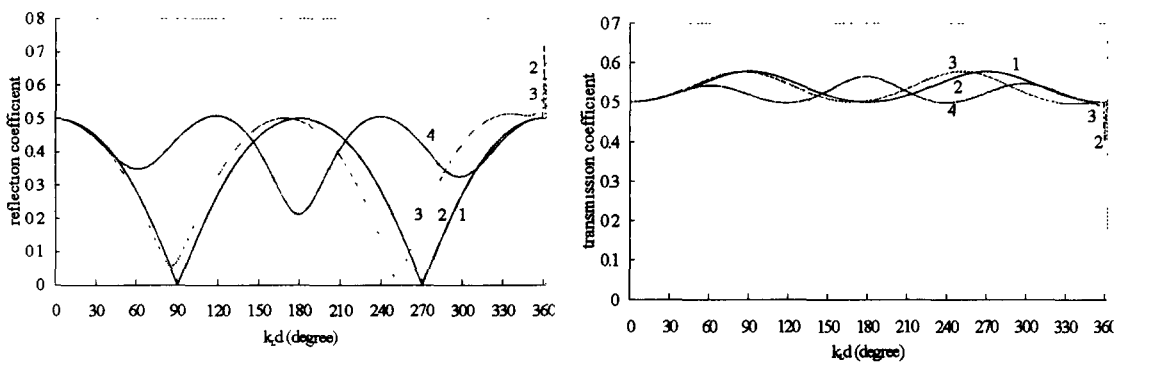

Fig.6 (a) reflection coefficient and (b) transmission coefficient for normally incident longitudinal waves versus k_Ld, curve 1: region 2 being achiral medium with $Z_2 = \sqrt{Z_1 Z_3}$, curve 2: $J\beta^2 k_L^2 k_{RL}^2 = 10^{-3}$, $k_{RL}/k_L = 0.5$, curve 3: $J\beta^2 k_L^2 k_{RL}^2 = 10^{-1}$, $k_{RL}/k_L = 0.5$, curve 4: $J\beta^2 k_L^2 k_{RL}^2 = 0.5$, $k_{RL}/k_L = 0.5$

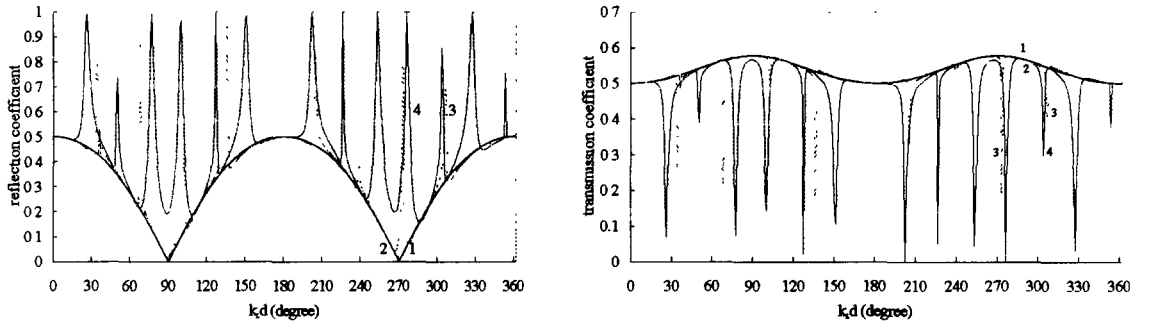

Fig.7 (a) reflection coefficient and (b) transmission coefficient for normally incident longitudinal waves versus $k_L d$, curve 1: region 2 being achiral medium with $Z_2 = \sqrt{Z_1 Z_3}$, curve 2: $J\beta^2 k_L^2 k_{RL}^2 = 10^{-3}$, $k_{RL}/k_L = 5$, curve 3: $J\beta^2 k_L^2 k_{RL}^2 = 10^{-1}$, $k_{RL}/k_L = 5$, curve 4: $J\beta^2 k_L^2 k_{RL}^2 = 0.5$, $k_{RL}/k_L = 5$

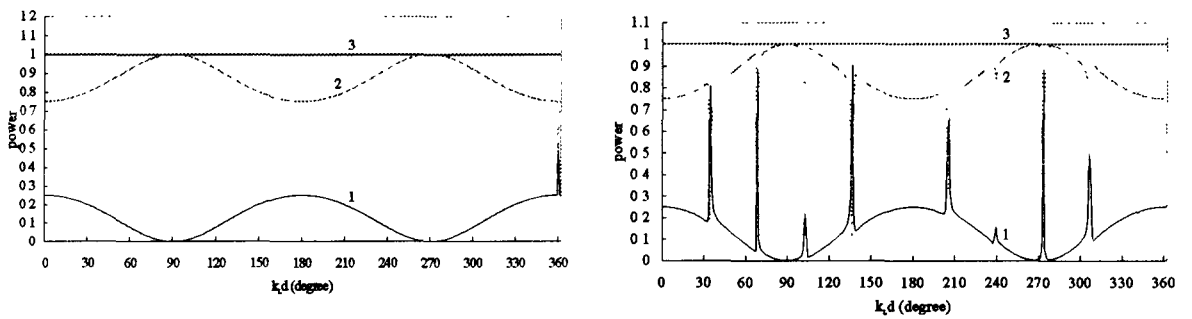

Fig.8 normalized power for normally incident longitudinal waves versus $k_L d$ with material constants: (a) $k_{RL}/k_{L2} = 0.5$, $J\beta^2 k_L^2 k_{RL}^2 = 10^{-3}$, and (b) $k_{RL}/k_{L2} = 5$, $J\beta^2 k_L^2 k_{RL}^2 = 10^{-1}$, curve 1: normalized reflected power, curve 2: normalized transmitted power and curve 3: total power